Electrostatic Forces and Molecular Transport in a Nanofountain Probe

Undergraduate Researcher
David J. Gebhart
Franklin W. Olin College of Engineering

Faculty Mentor
Horacio D. Espinosa
Department of Mechanical Engineering
Northwestern University

Graduate Student Mentor
Owen Y. Loh
Department of Mechanical Engineering
Northwestern University

Abstract
With the advent of a variety of novel nanometer-scale diagnostic techniques such as DNA micro- and nanoarrays, increasing focus has been placed on developing methods to quickly and accurately create these nanometer scale patterns. One promising technique for depositing DNA, proteins, and other liquid molecular "inks" with submicron resolution is the nanofountain probe (NFP). The NFP is a specially designed atomic force microscope cantilever that works like a microfluidic pen, transporting inks from a remote reservoir to the substrate. During patterning, a liquid ink meniscus forms between the probe's tip and the substrate. The shape of the meniscus, and thus the working resolution of the NFP, is dependent upon the properties of both the substrate and the ink. Ink transport can be aided by the forces created by an electrophoretic voltage. ANSYS finite element analysis software was used to model the forces created on the ink meniscus due to an applied voltage, and these forces were evaluated in their ability to modulate patterning resolution. A working qualitative model was created and used to evaluate the system for various meniscus geometries.

Introduction
Recent advances in biological detection assays — such as DNA micro- and nanoarrays and lab-on-a-chip microfluidic devices — have become invaluable in enhancing researchers' ability to detect and quantify very small samples. Such advances have improved sensitivity and reduced reagent costs.[1] These advances come alongside many new techniques for printing and patterning at the submicron scale.

Two of these techniques, dip pen nanolithography (DPN) and nanofountain probe lithography (NFP), use modified atomic force microscopy (AFM) cantilevers to deposit "inks," such as nanoparticles or proteins, onto the substrate.[1–3] In both of these techniques, the chief resolving factor is the size and shape of the water meniscus that forms between the tip and the surface due to ambient humidity.[2,4] An overview of these techniques is shown in Figure 1. Larger meniscuses allow the ink to pass onto a proportionally larger area of the surface, increasing line widths and reducing resolution.[4]

The transport of charged biological molecules within a liquid ink solution from the tip of the NFP onto the surface can be assisted by the introduction of an electric potential. The goal of this investigation was to create a computational model for the local effects of the electric field at the tip of the NFP.

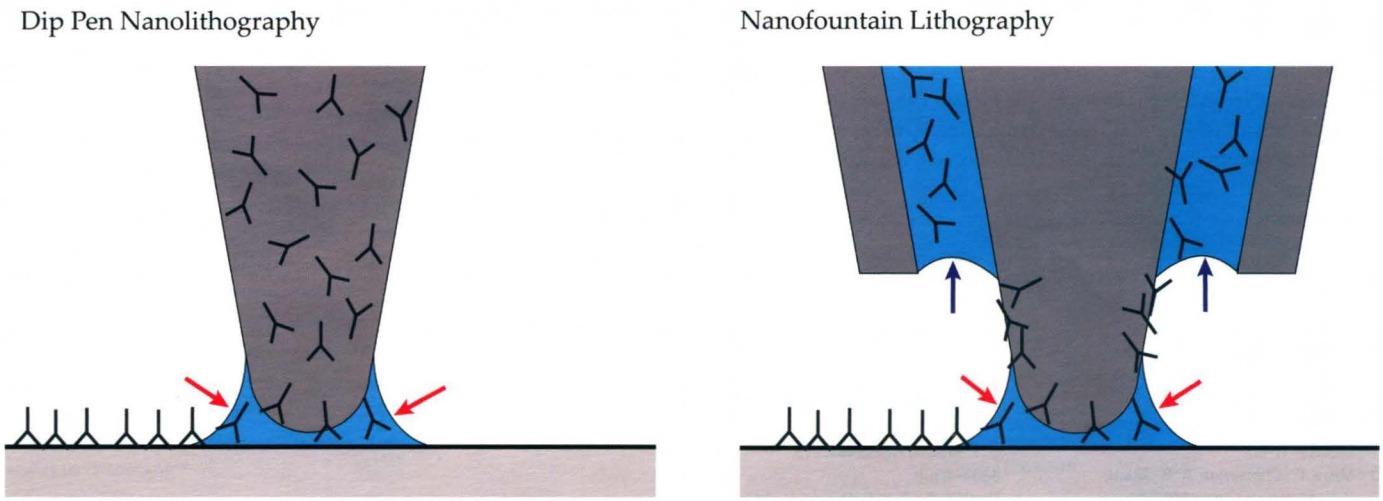

Figure 1. Schematic Representation of DPN and NFP nano-patterning techniques. Liquid ink meniscus is indicated by blue arrows, and humidity meniscus is shown with red.

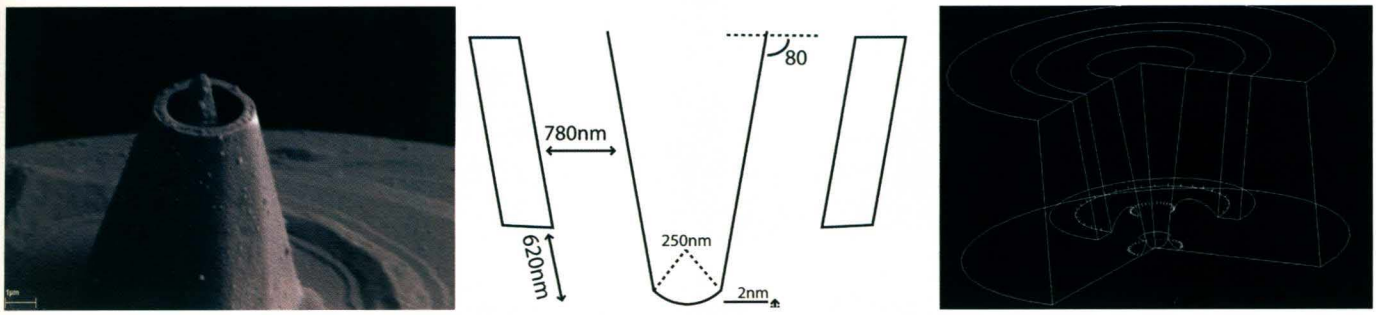

Figure 2. Physical and model representations of the system. From left to right, SEM image of NFP tip,[7] schematic of tip geometries, and symmetric expansion of the computational model.

Background

The first generation of cantilever-based nanolithography tools was developed when it was noticed that the tip of an atomic force microscope would leave an observable trail of water as it traveled very close (~1 nm) to the substrate being observed.[2,5] This trail was the result of a water meniscus spontaneously forming due to humidity in the microscope chamber.[5] This phenomenon was exploited in the creation of DPN, in which an AFM cantilever would be coated with ink, allowed to dry, and then placed nearly in contact with the surface.[2] The humidity meniscus that formed would then allow the transport of ink molecules onto the surface. This technique proved very effective at producing high-resolution pattering (<50 nm) with a variety of inks. However, DPN requires that the ink be dried on the probe tip, which must then be replenished once exhausted; for biological or other sensitive samples this could lead to changes in chemical behavior.

In order to work around these limitations, researchers developed the NFP. In this device the AFM cantilever, instead of being dipped in the pool of ink and allowed to dry, has a microfluidic channel connecting the tip to an external reservoir.[3] This reservoir continuously delivers ink to the tip, allowing rapid patterning for extended periods while maintaining the liquid state of the ink.[3] Thus, in addition to the small water meniscus formed in ambient humidity at the tip as in DPN, there is a liquid ink meniscus that is continuously fed by the microchannels (see Figure 1). This design is also conducive to parallelization through the use of multiple cantilevers connecting to different reservoirs, allowing simultaneous deposition of different inks.[6]

In an effort to consistently achieve sub-100 nm resolution, factors affecting patterning resolution have been investigated both experimentally and computationally.[1,2,4,7] One such factor is the varying shape of the meniscus created at the surface by the NFP tip. Early work simulating this meniscus focused primarily on surface energy calculations and did not consider the effects of a possible electric field used to help drive charged biological molecules onto the surface.[7] This investigation modeled and studied the possible effects of that electric field.

Approach

In order to explore the possible effects an electric field could have at the NFP tip, an electrostatic model was created using the finite element analysis software package ANSYS.[8] The geometry of the NFP tip was first recreated based on measurements from scanning electron microscopy images of actual probe tips. The liquid meniscus was then added based upon earlier simulations to determine this equilibrium geometry.

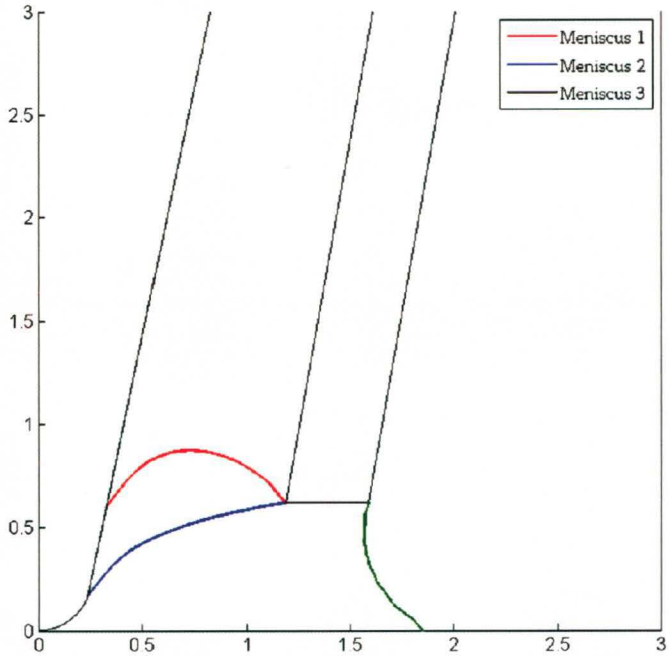

Figure 3. A comparison of the three meniscus shapes used in preliminary studies. Axes indicate position in units of microns.

Tip Geometry

The model geometry was derived from previous electron microscopy characterization of fabricated NFP devices, as shown in Figure 2.[3] From these schematic measurements, an ANSYS model was created using axisymmetric geometry, simplifying the simulation into two dimensions. The finite element used was the 2-D 8-node electrostatic element PLANE 121. A μMKS unit system was enforced on all measurements as well as constants.

Meniscus Geometry

Although the precise geometry of the cantilever tip is readily measured through electron microscopy observation, it is more difficult to directly observe the shape of the ink-air interface that forms at the tip during writing. To approximate this information, data for the meniscus geometry was obtained from previous work using the Surface Evolver software package.[7] The tool works by minimizing the surface energy at a defined model geometry with a given volume of liquid, yielding the equilibrium shape of the meniscus.[9] This raw data was then parsed and

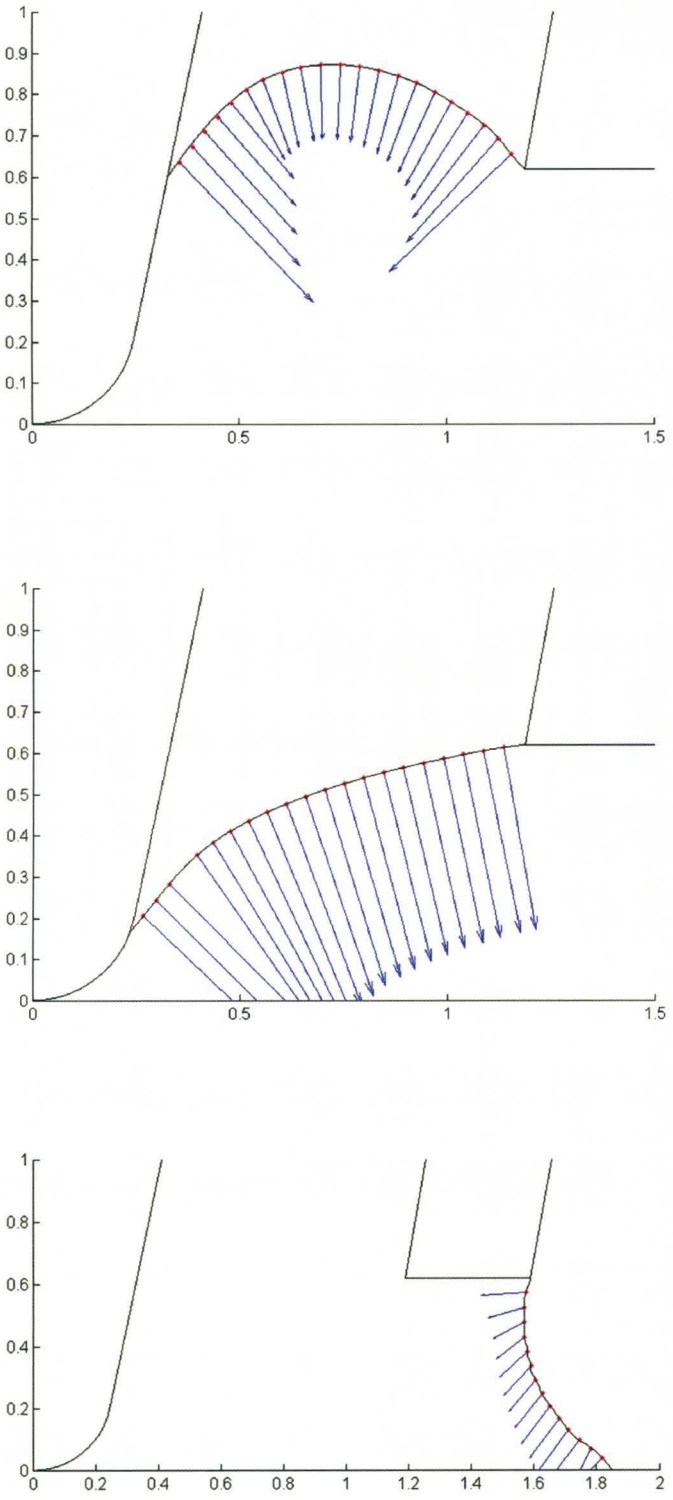

Figure 4. A comparison of calculated electric force vectors for the three studies' meniscus shapes. Axes indicate position in units of microns.

incorporated into the ANSYS model using a MATLAB script. Initially, three different meniscus geometries, corresponding to different liquid volumes, were used in the simulations (Figure 3). An additional investigation also considered the presence of the smaller humidity meniscus. This meniscus, formed at the base of the tip due to local humidity (as in DPN), was also modeled using the Surface Evolver package.

Modeling

Models were created using the ANSYS finite element analysis toolkit. In order to reduce the complexity of the simulation, an axisymmetric approximation was used along the central axis of the tip. This simplification closely approximates the symmetry of the conical tip.

In all experiments, voltage loads were modeled with ground on the lower boundary, representing the substrate. The electromotive voltage was modeled as a constant boundary voltage of 3V along the upper edge of the liquid within the tip. This is an approximation for the physical system in which the voltage is applied at the spatially distant reservoir and conducted through the microfluidic channels to the tip. This approximation was made based on the calculated resistance of the microchannels and the resulting voltage drop along them upon application of the voltage load. In this way the model remained qualitatively accurate and allowed quantitative approximation of electrostatic force. The model output voltage and electric field values for each node in the system were saved as text files and imported into MATLAB.

Work and Energy Analysis

After creating the general model for both voltage and electric field, the model was explored from the perspective of work and energy. Model information such as the electric field was exported as text from the ANSYS toolkit and imported into MATLAB. This imported data was then parsed and sorted, recreating the ANSYS-derived mesh into the more robust processing environment of MATLAB. From this raw data, the electric field data along the boundary of each meniscus were extracted. These field measurements were then equated on each node to electric pressures according to the expression $P_0 = \frac{1}{2} \varepsilon E^2$.[10] These pressures, representing the force applied by the electric field at the boundary of the conductive liquid, could change the configuration of the ink meniscus. Once the force on each node was established for each meniscus, this information was compared qualitatively between each of the meniscus geometries. Vectors representing the electric forces on the meniscus are shown in Figure 4. In a more quantitative calculation, the work done by the electric field moving the meniscus between different confirmations was calculated. Previous work established the surface energy for varying volumes of liquid within the tip geometry.[7] These different energies are plotted in Figure 5. For the work calculation, meniscus data for two adjacent volumes were modeled in the ANSYS software and electric force data were exported. Using this force data along with comparative geometries allowed for a simple work calculation wherein displacement was calculated between corresponding nodes and multiplied by the electric force.

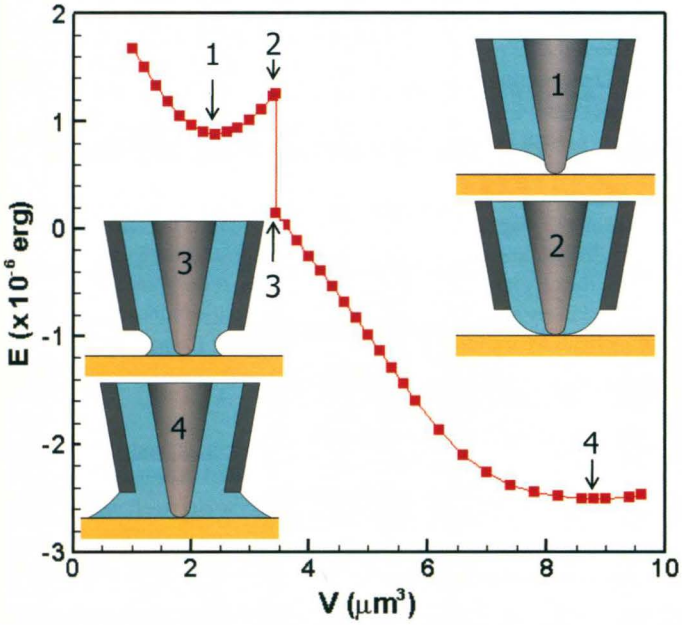

Figure 5. Surface energy calculated for varying volume of liquid within the NFP tip. (Image taken from Loh et al.)

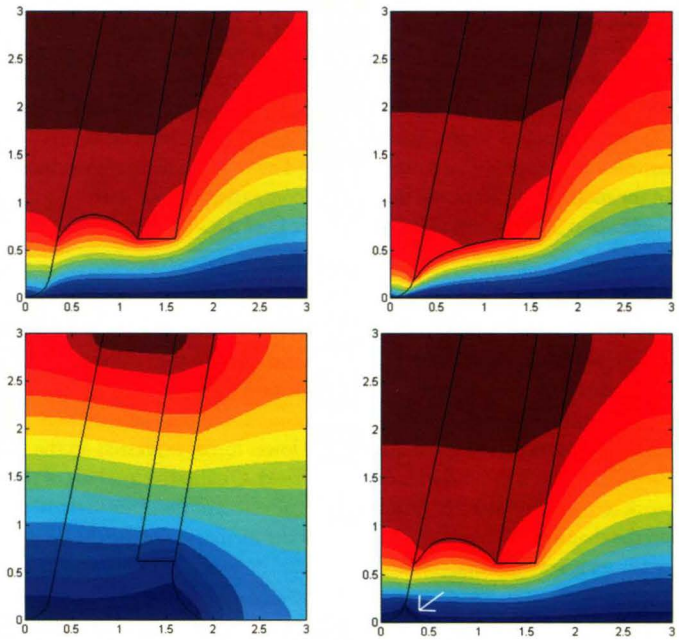

Figure 6. Comparison of Voltage contours for all studied meniscus shapes. The lower-right image demonstrates the result of the added humidity meniscus (large arrow). All contours go from 3V, red to 0V blue. Axes indicate position in units of microns.

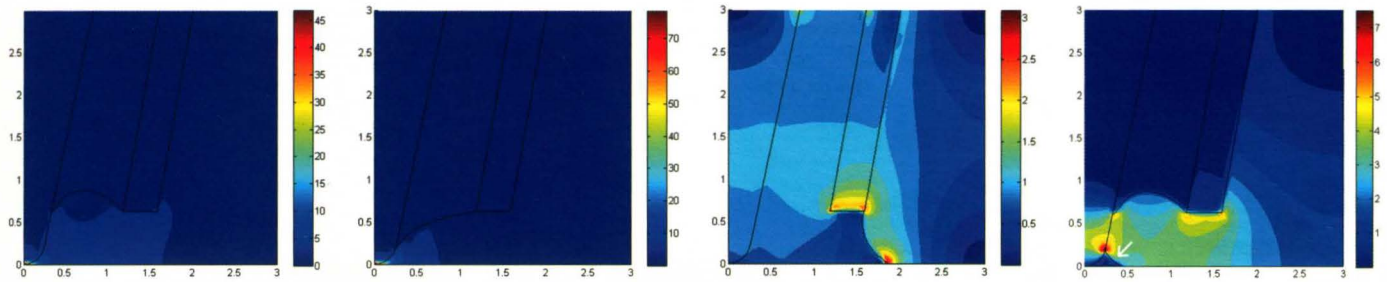

Figure 7. Comparison of electric field lines for all studied meniscus shapes, again the lower right image shows the addition of the humidity meniscus.

Results

Meniscus Shape

Voltage and electric field were compared between the three studied meniscus geometries. Voltage contours for all studied meniscus geometries are shown in Figure 6. In the first two cases, the meniscus was entirely contained within the shell of the tip, with a physical separation between the conductive liquid and the surface. Thus, the bulk of the voltage drop occurred in the air between the grounded surface and the nonconducting tip. Since this gap is relatively small and the voltage change at the tip is substantial, the area shows a very high electric field. This high field likely does not represent physical reality, as there will in fact be a small meniscus present at the tip-substrate interface due to ambient humidity as discussed below. This electric field peak is lost when transitioning to the third geometry, which shows the conductive liquid making contact with the lower boundary, leading to a more uniform voltage gradient and minimizing the electric field peaks, as seen in Figure 7.

Humidity Meniscus

The extreme electric field peaks, seen in the first images of Figure 7, were also eliminated through the addition of the humidity meniscus. This small band of conductive liquid in the air gap between the tip and the surface eliminated the large voltage gradient and smoothed the electric field. This model was a more accurate representation of the physical system, because the humidity-induced meniscus is present in all working variations of AFM cantilever nanopatterning.[1,2]

Electrostatic Force on Charged Biomolecules

Based on the magnitudes of the modeled electric fields, it was verified that they are adequate to produce a significant driving force on charged biomolecules within the ink solution. The model predicts electric fields of approximately 8 V/μm. Studies of DNA separation have been conducted at approximately 0.3 V/μm.[11] The lack of a resistant medium in the model does, however, limit direct comparison. Thus with application of the correct bias, the electric field does indeed aid molecular transport to the substrate.

Energy Analysis

The MATLAB script written to evaluate the forces on the meniscus was successful in picking out the nodes corresponding to the boundary and performing calculations with this data. These calculations showed several expected trends, such as (1) forces due to electric pressure oriented normal to the meniscus and (2) lower forces expressed on the meniscus, which showed a lesser electric field. Qualitative analysis of the work remains the focus of future work. The effect of these normal forces on the shape of the liquid-air interface of the meniscus will be the focus of future investigations.

Discussion

The model confirmed the prediction that the electrostatic forces generated by the applied voltage exert a significant force on the charged biomolecules within the liquid ink and thus aid transport to the substrate. These forces were approximately comparable to the forces experienced during other electric manipulation of biological molecules, such as gel electrophoresis separation of DNA. The model containing the physically accurate humidity meniscus predicted a peak electric field near the contact point of approximately 8 V/μm. If the ink is assumed to contain charged particles such as antibodies at a neutral pH, then this field indicates forces on the order of 10 pico-Newtons. This is comparable to the forces experienced during electrophoresis (DNA molecules have been shown to break at electrophoretic forces of approximately 50 pN). These results indicate that the model is an accurate predictor of biological molecule transport resulting from the electric field.

A key factor identified by this study is the significance of the interface between the tip and the substrate. The presence or absence of a conductive path of liquid between the tip and the substrate has dramatic effects on the shape of the voltage contours, and thus the electric field. In the first studies, where the liquid ink was constrained entirely within the tip, the very large electric field that resulted at the point of contact was most likely a consequence of an overly simplified model. These strong fields were eliminated with the inclusion of the more physically accurate humidity meniscus.

Conclusion

This work has served to create a qualitatively accurate model of the nanofountain probe. The model has demonstrated the capacity to evaluate simple quantities such as voltage and the electric field, as well as more complex data processing that shows force and work. The results of these calculations are ultimately limited by the accuracy of the assumptions used to create the model. This work has established a framework that will be expanded to provide insight into methods by which the resolution of NFP patterning may be improved and, with additional model complexity, the dynamics of the deposition process.

This research was supported primarily by the Nanoscale Science and Engineering Initiative of the National Science Foundation under NSF award number ***EEC – 0755375****. Any opinions, findings and conclusions or recommendations expressed in this material are those of the author(s) and do not necessarily reflect those of the National Science Foundation.*

References

1 Kim, K.-H.; Sanedrin, R. G.; Ho, A. M.; Lee, S. W.; Moldovan, N.; Mirkin, C. A.; Espinosa, H. D. *Adv. Materials* **2008,** *20,* 330–334.

2 Piner, R. D.; Zhu, J.; Xu, F. *Science* **1999,** *283,* 661.

3 Moldovan, N.; Kim, K.-H.; Espinosa, H. D. *J. Microelectromech. Systems* **2006,** *15,* 204–213.

4 Wu, B.; Ho, A.; Moldovan, N.; Espinosa, H. D. *J. Am. Chem. Soc.* **2007,** *23,* 9120–9123.

5 Xu, L.; Lio, A.; Hu, J.; Ogletree, F.; Salmeron, M. *J. Phys. Chem.* **1998,** *102,* 540–548.

6 Moldovan, N.; Kim, K.-H.; Espinosa, H. D. *J. Micromech. and Microeng.* **2006,** *16,* 1935–1942.

7 Loh, O.Y.; Ho, A. M.; Rim, J. E.; Kohli, P.; Patankar, N. A.; Espinosa, H. D. *Proc. Natl. Acad. Sci.* Submitted for publication 2008, *ANSYS®Academic Research, version 10.0.*

8 Brakke, K. A. *Exper. Math.* **1996,** *1,* 141–165.

9 Wright, G. S.; Krein, P. T.; Chato, J. C. *IEEE Transactions on Industry Applications* **1990,** *26,* 42–49.

10 Geoun, M. B.; Choi, K. S.; Lee, Y.-I.; Kim, Y. *Microchem. J.* **2002,** *72,* 305–313.

11 Gurrieri, S.; Smith, S. B.; Bustamante, C. *Proc. Natl. Acad. Sci.* **1999,** *96,* 453–458.